Journal of Electromagnetic Analysis and Applications, 2023, 15, 1-11
https://www.scirp.org/journal/jemaa
ISSN Online: 1942-0749
ISSN Print: 1942-0730

Radio Frequency Quadrupole for Bunching Electron Beam: Electromagnetic Field, Particle Velocity Range, and Accuracy at 10 GHz

Serigne Bira Gueye

Department of Physics, Faculty of Sciences and Techniques, Cheikh Anta Diop University, Dakar, Senegal
Email: bira.gueye@ucad.edu.sn

How to cite this paper: Gueye, S.B. (2023) Radio Frequency Quadrupole for Bunching Electron Beam: Electromagnetic Field, Particle Velocity Range, and Accuracy at 10 GHz. *Journal of Electromagnetic Analysis and Applications*, **15**, 1-11.
https://doi.org/10.4236/jemaa.2023.151001

Received: December 7, 2022
Accepted: January 17, 2023
Published: January 20, 2023

Copyright © 2023 by author(s) and Scientific Research Publishing Inc.
This work is licensed under the Creative Commons Attribution International License (CC BY 4.0).
http://creativecommons.org/licenses/by/4.0/
Open Access

Abstract

The Radio Frequency Quadrupole (RFQ) accelerator invented by Kapchinskii and Tepliakov can focus, bunch, and accelerate charged-particle beams simultaneously. Typically, it operates at frequencies up to 500 MHz, for low particle velocities ($\beta < 0.12$). The first attempt to design cylindrical RFQ for electrons in the GHz region was done using 3 GHz at Frascati in 1990. In this paper, an analytical approximation of the electromagnetic field is given, and linearized in the beam region for a rectangular Electron Radio Frequency Quadrupole (ERFQ). The differences between the proton-RFQ and the electron-RFQ are discussed. Then, it will be shown that contrary to the quadrupoles for protons or heavy-ions, the ERFQ is suited for electron velocities in the range 0.5 - 0.7 c, and possible applications are given. Finally, it is illustrated, with numerical field computations that this approach gives sufficient accuracy at 10 GHz.

Keywords

Electron RF Quadrupole, Buncher, Linear Accelerator, Linac, Beam Injector

1. Introduction

First, we show how the ERFQ can focus and accelerate particles. Then, an approximation of the electromagnetic field is done for a rectangular standing wave structure, in the GHz region. The linearization of this analytical solution allows us to obtain the potential function from which we deduce the geometry of the electrodes. The focusing efficiency of the structure is determined and discussed. It will be shown that the Electron-RFQ is suited for input beam velocities in the range of 0.5 - 0.7 c. Lastly, the accuracy of this approach is determined using the

program *GdfidL* [1] at 10 GHz.

2. Operating Principle of the ERFQ

2.1. Focusing

The RF Quadrupole is a waveguide composed of four electrodes. The two adjacent ones have opposite potentials. If we place electric walls on its diagonals, and magnetic walls on the other planes of symmetry, its electromagnetic propertie will not change. As a result, one needs to compute only an eighth of the whole unmodulated RFQ (see Figure 1).

During one RF half cycle, it focuses particles in one transverse plane while it defocuses them in another one. The gradient of the electric field is

$$G_o = \frac{V_0}{a^2}\sin(\omega t), \tag{1}$$

where a designates the *aperture radius* and V_0 the *inter-vane voltage*. After each half cycle, the sign of the gradient changes. We get an *Alternating Gradient Focusing* (AGF) channel that allows particle transport over a long distance through a small bore. According to the theory of AGF, a net focusing effect will occur in both transverse planes, resulting in the confinement of particle beams [2] [3] [4] [5] [6].

2.2. Emergence of an Axial Field E_z

The RFQ described above cannot accelerate particles if the electrode surfaces do not change along the z-axis. This is due to the fact that it does not have an axial

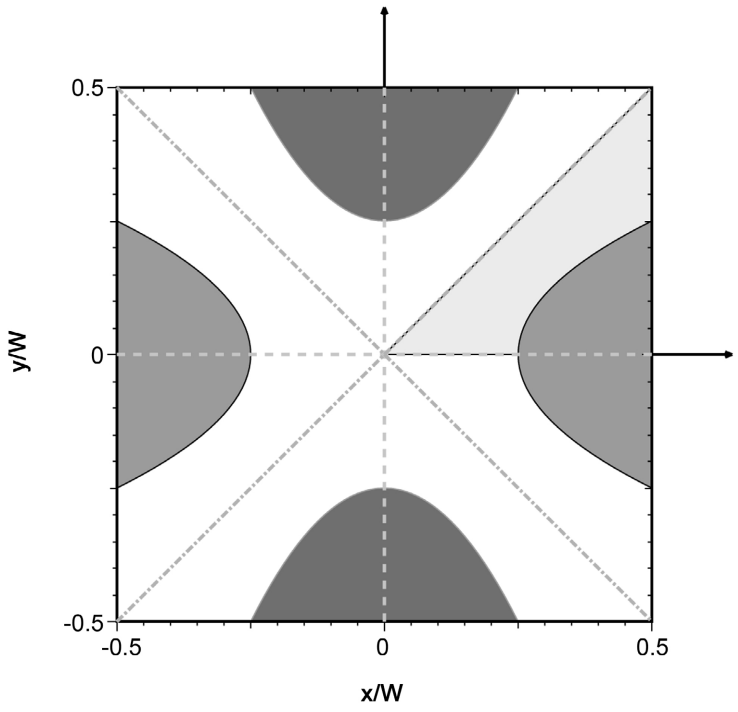

Figure 1. RF Quadrupole.

electric field. Therefore, we have to modulate the vanes with a displacement of the one-half period between two adjacent electrodes (see **Figure 2**) [2]-[7].

Here, the *cell length* is defined as the half modulation period. The *modulation factor m* is the fraction of the maximum distance between the vane and the axis to the minimum distance.

3. Field Approximation in GHz Region

For frequencies greater than 1 GHz, $\lambda_0 \gg a$ no longer holds and the wave equation has to be solved. The field is composed of two parts. The first one is the focusing part without acceleration, and the second one is the defocusing part with an axial electric field. The approach is the following:

- First, we approximate the focusing field with a TE mode, considering an unmodulated structure.
- Secondly, we consider a TM mode produced by the modulation [7].
- Lastly, we linearize the ERFQ field in the beam region.

The approximation is done for the main space harmonic, which interacts strongly with the particles.

3.1. TE Wave as Focusing Field

We are interested in one mode with quadrupole symmetry that focuses particles. Thus, for a transverse offset Δ, one gets $E_x(\Delta,0,z) = -E_y(0,\Delta,z)$. With the

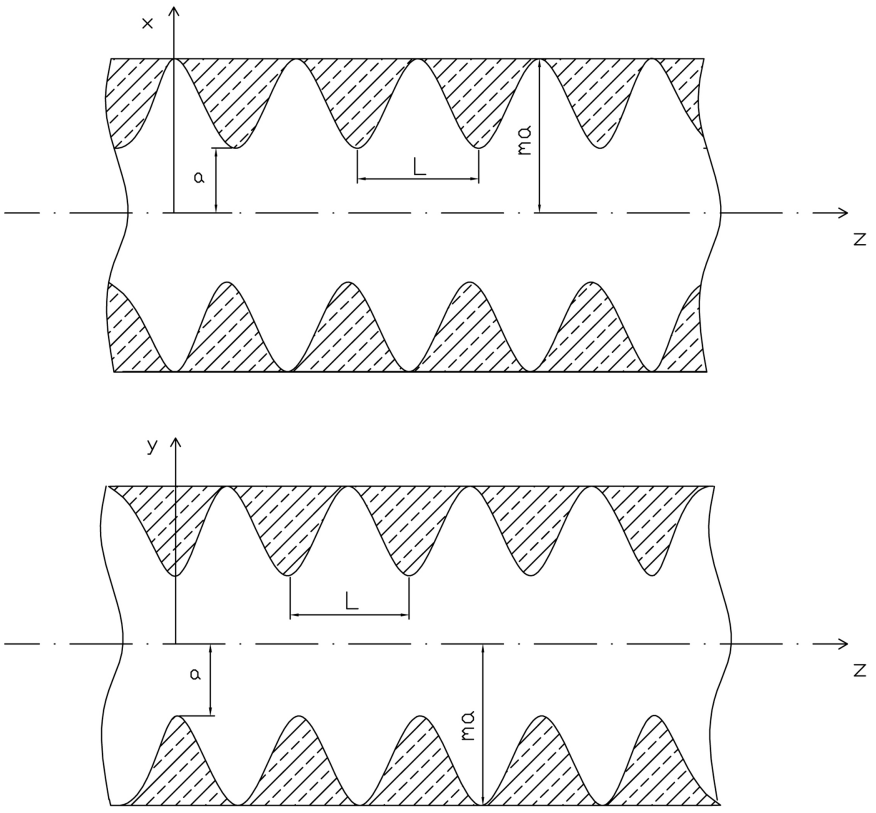

Figure 2. Vane modulation.

Bernoulli approach, it holds

$$E_x = X(x)Y'(y)Z(z)T(t) \text{ and } E_y = -X'(x)Y(y)Z(z)T(t). \quad (2)$$

The potential of the electrodes is $\pm\frac{V_0}{2}\sin(\omega t)$ and does not depend on z. That is why we can neglect the z-dependence in (2): $Z(z) = 1$. The solution of the wave equation is a modified TE11 mode. The modification comes from the capacitive loading of the empty waveguide with electric quadrupole vanes. We get the following electric field components

$$\begin{aligned} E_x^{TE} &= -\frac{\sqrt{2}}{k_0}A_{00}V_0\sin\left(\frac{k_0}{\sqrt{2}}x\right)\cos\left(\frac{k_0}{\sqrt{2}}y\right)\sin(\omega t) \\ E_y^{TE} &= +\frac{\sqrt{2}}{k_0}A_{00}V_0\cos\left(\frac{k_0}{\sqrt{2}}x\right)\sin\left(\frac{k_0}{\sqrt{2}}y\right)\sin(\omega t) \\ E_z^{TE} &= 0, \end{aligned} \quad (3)$$

where k_0 is the free space wave number. From Faraday's law, we can derive the magnetic field which only has a z-component

$$B_z^{TE} = -\frac{2}{\omega}A_{00}V_0\sin\left(\frac{k_0}{\sqrt{2}}x\right)\sin\left(\frac{k_0}{\sqrt{2}}y\right)\cos(\omega t). \quad (4)$$

3.2. Axial Electric Field with the Vane Modulation

The modulation of the vanes will create an axial electric field. The quadrupolar symmetry must be conserved. The divergence of $\tilde{E}$ vanishes, since there are no charges in the free space inside the structure. Therefore, the field generated by the modification of the electrodes can be approximated with:

$$\begin{aligned} E_x^{Mod} &= -\frac{\sqrt{2}}{k_c}A_{10}V_0\sin\left(\frac{k_c}{\sqrt{2}}x\right)\cos\left(\frac{k_c}{\sqrt{2}}y\right)\cos(k_z z)\sin(\omega t) \\ E_y^{Mod} &= -\frac{\sqrt{2}}{k_c}A_{10}V_0\cos\left(\frac{k_c}{\sqrt{2}}x\right)\sin\left(\frac{k_c}{\sqrt{2}}y\right)\cos(k_z z)\sin(\omega t) \\ E_z^{Mod} &= +\frac{2}{k_z}A_{10}V_0\cos\left(\frac{k_c}{\sqrt{2}}x\right)\cos\left(\frac{k_c}{\sqrt{2}}y\right)\sin(k_z z)\sin(\omega t), \end{aligned} \quad (5)$$

where k_c is the cut-off wave number and k_z the axial spatial frequency. The ERFQ field is obtained after superposition: $\tilde{E} = \tilde{E}^{TE} + \tilde{E}^{Mod}$, $\tilde{B} = \tilde{B}^{TE} + \tilde{B}^{Mod}$, with the dispersion equation $k_c^2 + k_z^2 = k_0^2$.

3.3. Field Linearization in the Beam Region

By assuming that the beam radius is very small, the following linear approximation can be done, in the beam region:

$$\sin\left(\frac{k_0}{\sqrt{2}}x\right), \sin\left(\frac{k_c}{\sqrt{2}}x\right) \approx \frac{k_0}{\sqrt{2}}x, \frac{k_c}{\sqrt{2}}x, \sin\left(\frac{k_0}{\sqrt{2}}y\right), \sin\left(\frac{k_c}{\sqrt{2}}y\right) \approx \frac{k_0}{\sqrt{2}}y, \frac{k_c}{\sqrt{2}}y$$

$$\cos\left(\frac{k_0}{\sqrt{2}}x\right), \cos\left(\frac{k_c}{\sqrt{2}}x\right) \approx 1, \text{ and } \cos\left(\frac{k_0}{\sqrt{2}}y\right), \cos\left(\frac{k_c}{\sqrt{2}}y\right) \approx 1.$$

In this case, the field in the RFQ can be written:

$$\begin{aligned} E_x &= -V_0 x\left[+A_{00} + A_{10}\cos\left(k_z z\right)\right]\sin\left(\omega t\right) \\ E_y &= +V_0 y\left[+A_{00} - A_{10}\cos\left(k_z z\right)\right]\sin\left(\omega t\right) \\ E_z &= +\frac{2}{k_z}A_{10}V_0\sin\left(k_z z\right)\sin\left(\omega t\right). \end{aligned} \tag{6}$$

Taking the induction law $\tilde{\nabla}\times\tilde{E} = -\dfrac{\partial\tilde{B}}{\partial t}$ with the synchronism condition $k_z = \dfrac{w}{bc}$, we obtain the magnetic field components

$$\begin{aligned} \beta c B_x &= -A_{10}V_0 y\sin\left(k_z z\right)\cos\left(\omega t\right) \\ \beta c B_y &= +A_{10}V_0 x\sin\left(k_z z\right)\cos\left(\omega t\right) \\ \beta c B_z &= 0 \end{aligned} \tag{7}$$

or in cylindric coordinate system $\beta c\tilde{B} = A_{10}V_0\rho\sin\left(k_z z\right)\cos\left(\omega t\right)\tilde{e}_\varphi$.

4. Potential Function and Vane Shaping

4.1. Potential Function

The following potential function can be derived from the components of the electric field:

$$U\left(x,y,z,t\right) = U_r\left(x,y,z\right)\sin\left(\omega t\right) \quad \text{with} \tag{8}$$

$$U_r\left(x,y,z\right) = \frac{V_0}{2}\left[\left(x^2 - y^2\right)A_{00} + \left(x^2 + y^2 + \left(\frac{2}{k_z}\right)^2\right)A_{10}\cos\left(k_z z\right)\right]. \tag{9}$$

One sees that

$$-\frac{\partial U}{\partial z} = E_z + \frac{k_z}{2}A_{10}V_0\left(x^2 + y^2\right)\sin\left(k_z z\right)\sin\left(\omega t\right). \tag{10}$$

With the magnetic vector potential $\tilde{A}$, one has $\tilde{E} = -\tilde{\nabla}U - \dfrac{\partial\tilde{A}}{\partial t}$. It follows that

$$\frac{\partial\vec{A}}{\partial t} = \frac{k_z}{2}A_{10}V_0\left(x^2 + y^2\right)\sin\left(k_z z\right)\sin\left(\omega t\right)\vec{e}_z, \tag{11}$$

$$\beta_s c\vec{A} = -\frac{1}{2}A_{10}V_0\left(x^2 + y^2\right)\sin\left(k_z z\right)\cos\left(\omega t\right)\vec{e}_z. \tag{12}$$

These results can be shown to satisfy $\tilde{B} = \tilde{\nabla}\times\tilde{A}$.

4.2. Vane Shaping

The electrodes build equipotential surfaces on which the potential function satisfies the following requirements

$$U\left(x,y,z,t\right) = \pm\frac{V_0}{2}\sin\left(\omega t\right). \tag{13}$$

As shown before in **Figure 2**, it holds for a modulation factor m

$$U_r(a,0,0) = +\frac{V_0}{2} \text{ and } U_r(0,ma,0) = -\frac{V_0}{2}. \quad (14)$$

A_{00} and A_{10} are given by:

$$A_{00}a^2 = \frac{\left(m^2+1\right)+\frac{2}{\pi^2}\left(\beta\frac{\lambda_0}{a}\right)^2}{2m^2+\frac{m^2+1}{\pi^2}\left(\beta\frac{\lambda_0}{a}\right)^2}0 \text{ and } A_{10} = \frac{m^2-1}{2m^2+\frac{m^2+1}{\pi^2}\left(\beta\frac{\lambda_0}{a}\right)^2}. \quad (15)$$

If the three parameters $\frac{\lambda_0}{a}$, β, and m are known, the vane surfaces can be designed by solving Equation (13).

4.3. Interpretation of the RFQ Parameters A_{00} and A_{10}

We can observe that the two parameters A_{00} and A_{10} have great importance for the RFQ. A_{00} is related to the focusing and A_{10} is associated with the acceleration. Let us consider the quadrupole without vane modulation. From (1), the gradient of the electric field is $G_o = \frac{V_0}{a^2}\sin(\omega t)$. With the modulation, the gradient becomes

$$G_m = A_{00}V_0\sin(\omega t). \quad (16)$$

The *focusing efficiency* χ of the RFQ can be defined to be the factor that determines how good the quadrupole with modulation focuses in comparison to the unmodulated cavity:

$$\chi = \frac{G_m}{G_o} = A_{00}a^2. \quad (17)$$

The inequality $0 < \chi \le 1$ can be deduced. With the vane modulation, the acceleration increases and the focusing efficiency decreases. From (14), the following is derived

$$\chi + \underbrace{\left(a^2+\left(\frac{2}{k_z}\right)^2\right)}_{:=A_{cc}}A_{10} = 1. \quad (18)$$

Defining A_{cc} as the *acceleration efficiency*, (18) yields the following equation $\chi + A_{cc} = 1$. We see that: If χ decreases, A_{cc} increases and vice versa.

5. Electron-RFQ Is Suited for $0.5 \le \beta \le 0.7$

The normalized velocity β alone does not determine the efficiency of the RFQ. Equations (15) and (17) show that for a given modulation factor m, the focusing efficiency χ of the RFQ depends on the very important term $\beta\frac{\lambda_0}{a}$. It is true that the proton and heavy-ion RFQs are suited for low beam velocities (typically $\beta < 0.12$). However, they operate at frequencies for which it holds $\frac{\lambda_0}{a} \gg 1$. For

example, an ion-RFQ works at 200 MHz with an average aperture radius a = 0.4 cm, an output energy of 1750 keV ($\beta = 0.0610$), and a final modulation factor $m = 2$. It holds, for this structure $\frac{\lambda_0}{a} = 375$, and one gets at its output $\beta \cdot \frac{\lambda_0}{a} \approx 22.9$ and $\chi \approx 40.7\%$ (see **Figure 3**).

The electron-RFQ that we propose differs from the proton and heavy-ion RFQs in some important aspects. Firstly, it operates at frequencies higher than 1 GHz with $\frac{\lambda_0}{a} < 7$. Secondly, in this frequency range, the inter-vane voltage is much lower than that of proton devices. Thirdly, we have the difference of mass between electron and proton. Another important aspect is that electrons are already emitted from a typical gun source with velocities approaching half the speed of light ($\beta \approx 0.5$) [8].

From all these considerations, we deduce that the electron-RFQ will be designed in four sections. But, it works differently with respect to the structures for heavy-ion or proton. The electron-RFQ can work for $0.5 \le \beta \le 0.7$, contrary to the quadrupole for protons and heavy-ions. It can have the following applications:

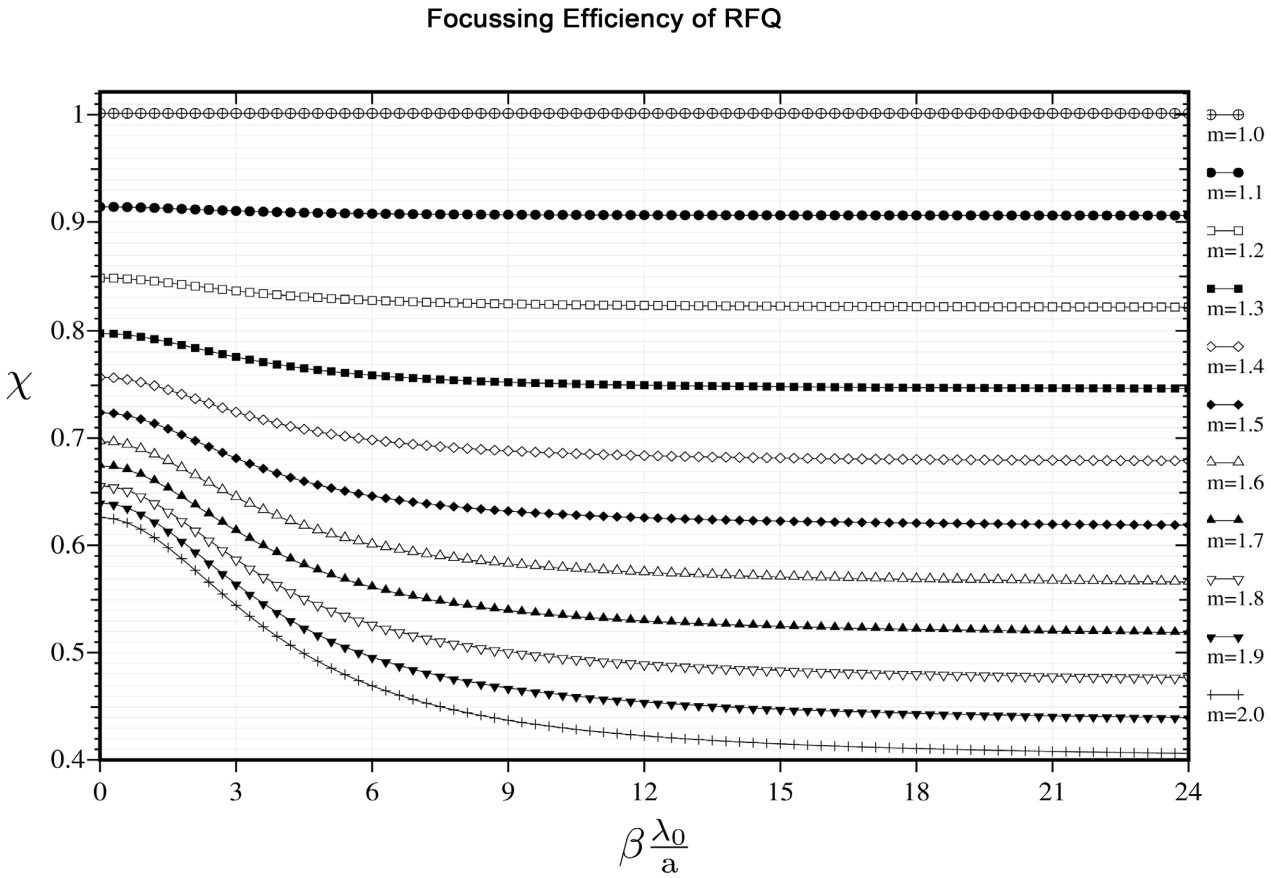

Figure 3. Focusing efficiency χ as function of $\beta \frac{\lambda_0}{a}$.

- Since the ERFQ has a Shaper and a Buncher, it can work as a prebuncher and buncher, after an rf gun. In this case, the input normalized beam velocity is $\beta \approx 0.5$ [9].
- The electron-RFQ can work as a standing wave buncher, in a bunching section of a preinjector linac, after a subharmonic prebuncher (a TM_{010} pillbox cavity) and a triode electron gun. In this case, the ERFQ is partially embedded in a focusing solenoid (input $\beta \approx 0.7$) [9] [10].

For electron, the ERFQ acceleration efficiency is not high, even with a quadrupole acceleration section [11]. For electron acceleration, there are more efficient devices. However, it is a very good buncher for continuous electron beam. It also has the following advantages: large bandwidth, symmetrical beam handling in the transverse direction. It can be fabricated, even at very high frequencies, in four parts, using the micro-machining technology LIGA that consists of Deep-etched X-ray Lithography (DXRL), electroplating, and micro-molding [12] [13] [14].

6. Accuracy of the Approximation at 10 GHz

It is important to know how good our analytical field approximation is. For this reason, we consider an ERFQ with modulated vanes (see Figure 4). The electrode tips that build equipotential surfaces are plotted from Equation (13). The modulation factor is $m = 1.7$. The structure is quadratic with width $w = 8.0169$

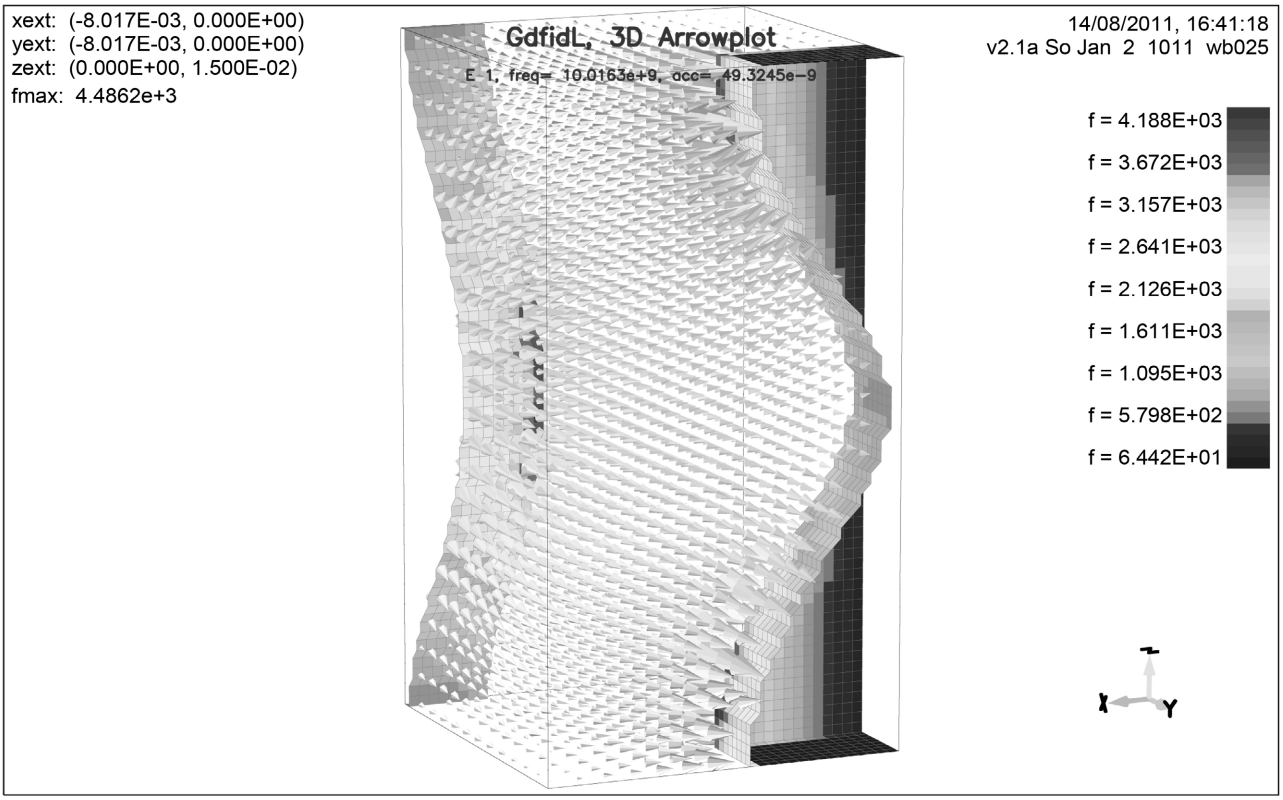

Figure 4. One fourth of an ERFQ cavity.

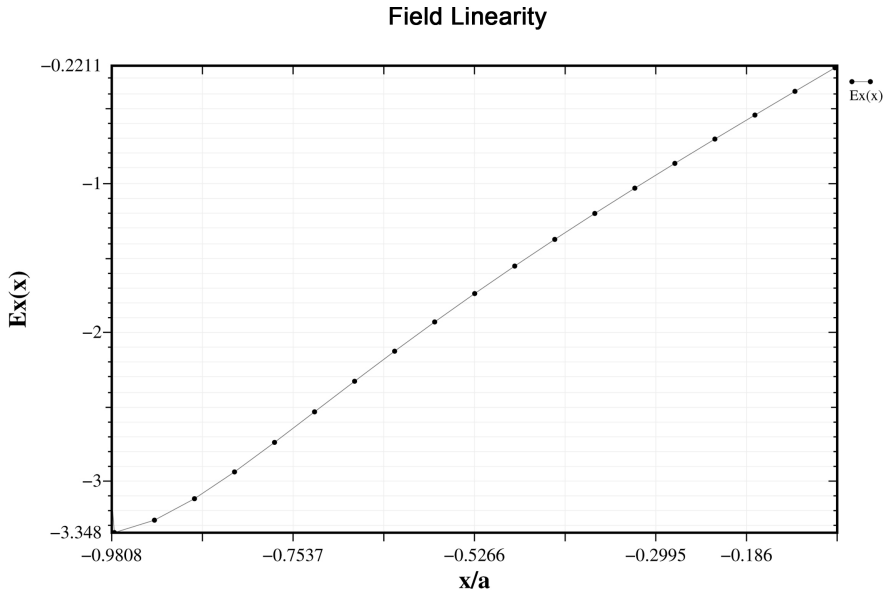

Figure 5. Field linearity.

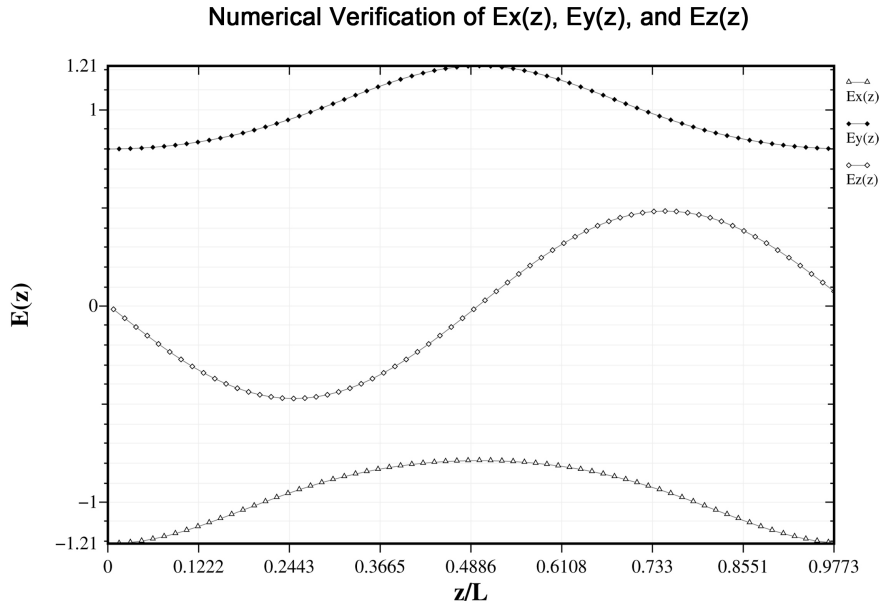

Figure 6. Numerical verification of $E_x(z)$, $E_y(z)$, and $E_z(z)$.

mm and its aperture radius is $a = 4.5696$ mm. With the program *GdfidL*, the 2π mode is computed over one period $L = \beta\lambda_0$, at 10 GHz, for a normalized phase velocity $\beta = 0.5$. The planes $x = 0$, $y = 0$, $z = 0$, and the plane $z = L$ represent magnetic walls: the fourth of the modulated ERFQ is sufficient for numerical computations.

Figure 4 confirms that we have an AGF channel. We can see, an electrode focusing the particles in one transverse plane while the adjacent vane defocuses them in another plane.

In Figure 5, we plot with the post-processor of *GdfidL* the x-component of

the electric field $E_x(x) := \frac{E_x(x,0,0)}{\Delta A_{00} V_0}$, for an offset $\Delta = 1.8278$ mm. The field shows a linearity for $-0.9273a < x, y < 0$: our approximation is good enough for a beam radius $r_b < 0.9273a$. Therefore, the field linearization in the beam region is correct, although a linear function is not a solution of the wave equation.

In **Figure 6**, we have the functions $E_x(z) := \frac{E_x(-\Delta,0,z)}{\Delta A_{00} V_0}$, $E_y(z) := \frac{E_y(0,-\Delta,z)}{\Delta A_{00} V_0}$, and $E_z(z) := \frac{E_z(0,0,z)}{\Delta A_{00} V_0}$: they have the form described by Equation (6). We deduce that our approach is good. It has the advantage to give us the electromagnetic field with sufficient accuracy.

7. Conclusion

This paper has provided an analytical study of the electromagnetic field of a rectangular radio frequency quadrupole. The obtained solution has been linearized, with good accuracy, in beam-region, for frequencies higher than 1 GHz. We have seen that an RFQ is an efficient prebuncher or buncher for a continuous electron beam, and its acceleration efficiency is low. In a next article, we will present the results of beam simulations with the Particle-in-Cell Method.

Conflicts of Interest

The author declares no conflicts of interest regarding the publication of this paper.

References

[1] Bruns, W. (1996) GdfidL: A Finite Difference Program for Arbitrarily Small Perturbations in Rectangular Geometries. *IEEE Transactions on Magnetics*, **32**, 1453-1456.

[2] Kapchinskii, I.M. and Tepliakov, V.A. (1970) Linear Ion Accelerator with Spatially Homogeneous Strong Focusing. *Pribory i Tekhnika Eksperimenta*, **2**, 19-22.

[3] Stanley Humphries, Jr. (1986) Principles of Charged Particle Acceleration. John Wiley & Sons, New York.

[4] Weiss, M. (1987) Radio Frequency Quadrupole. CERN Accelerator School, Aarhus.

[5] Puglisi, M. (1985) The Radio Frequency Quadrupole Linear Accelerator. CERN Accelerator School, Oxford.

[6] Wangler, T.P. (1996) Strong Focusing and Radio-Frequency Quadrupole Accelerator. *American Journal of Physics*, **64**, 177-182. https://doi.org/10.1119/1.18300

[7] Picardi, L., Raimondi, P. and Ronsivalle, C. (1991) Study of the Electromagnetic Fields in an Electron RFQ Structure. *Nuclear Instruments and Methods in Physics Research Section A*: *Accelerators*, *Spectrometers*, *Detectors and Associated Equipment*, **303**, 209-214. https://doi.org/10.1016/0168-9002(91)90790-W

[8] Wangler, T.P. (1998) Principles of RF Linear Accelerators. John Wiley & Sons, New York, 232. https://doi.org/10.1002/9783527618408

[9] Wang, S.H. (1990) RF Electron Linac. Lecture Note, 16-17, Institute of High Energy Physics (IHEP), Beijing, China.

[10] D'Auria, G., *et al.* (2008) Installation and Commissioning of the 100 MeV Preinjector Linac of the New Elettra Injector. *Proceedings of EPAC* 2008, Genoa, 23-27 June 2008, 2160-2162.

[11] Picardi, L., Raimondi, P. and Ronsivalle, C. (1990) Electron-RFQ: A Possible Novel Electron High Brightness Current Injector. *EPAC* 90, Nice, 12-16 June 1990, 682-684.

[12] Kroll, N.M., *et al.* (1999) Planar Accelerator Structures for Millimeter Wavelengths. *Proceedings of the* 1999 *Particle Accelerator Conference*, New York, 29 March-2 April 1999, 3612-3614.

[13] Kustom, R.L., Feinerrnan, A.D., Grudzien, D., *et al.* (1994) Microcavity Structures. 17*th International Linear Accelerator Conference* (*LINAC* 94), Tsukuba, 21-26 August 1994.

[14] Song, J.J., Bajikar, S., Decarlo, F., *et al.* (1998) LIGA-Fabricated Compact mm-Wave Linear Accelerator Cavities. *Microsystem Technologies*, **4**, 193-196. https://doi.org/10.1007/s005420050129